DMD Fast Forward. Published on April 26, 2019 as DOI: 10.1124/dmd.119.087007
This article has not been copyedited and formatted. The final version may differ from this version.

Indinavir increases midazolam *N*-glucuronidation in humans: identification of an alternate CYP3A inhibitor using an in vitro to in vivo approach

Dan-Dan Tian, Cathrine Leonowens[1], Emily J. Cox[2], Vanessa González-Pérez[3], Kosea S. Frederick[4], Yolanda V. Scarlett, Michael B. Fisher[†], and Mary F. Paine

Department of Pharmaceutical Sciences, Washington State University, Spokane, WA (D.D.T., E.J.C., V.G.-P., M.F.P.); Division of Gastroenterology and Hepatology, School of Medicine (Y.V.S.), and Division of Pharmacotherapy and Experimental Therapeutics, Eshelman School of Pharmacy (C.L.), The University of North Carolina at Chapel Hill, Chapel Hill, NC; Boehringer-Ingelheim Pharmaceuticals, Inc., Ridgefield, CT (K.S.F., M.B.F.)

DMD Fast Forward. Published on April 26, 2019 as DOI: 10.1124/dmd.119.087007
This article has not been copyedited and formatted. The final version may differ from this version.

Running title: midazolam *N*-glucuronidation increases in the presence of indinavir

Corresponding author:

Mary F. Paine, RPh, PhD

PBS 341, PO Box 1495

College of Pharmacy and Pharmaceutical Sciences

Washington State University

Spokane, WA 99210-1495

Telephone: 509-358-7759

FAX: 509-368-6673

E-mail: mary.paine@wsu.edu

Number of:

Text pages: 16

Tables: 2

Figures: 8

References: 22

Words in *Abstract*: 248

Words in *Introduction*: 576

Words in *Discussion*: 852

Abbreviations: AUC, area under the plasma concentration versus time curve; C_{max}, maximum plasma concentration; CYP, cytochrome P450; DDI, drug-drug interaction; HLMs, human liver microsomes; UDPGA, uridine 5'-diphosphoglucuronic acid ammonium salt; rCYP3A4, recombinant CYP3A4; rUGT1A4, recombinant UGT1A4; SPE, solid phase extraction

Abstract

Midazolam is a widely used index substrate for assessing effects of xenobiotics on CYP3A activity. A previous study involving human hepatocytes showed the primary route of midazolam metabolism, 1'-hydroxylation, shifted to *N*-glucuronidation in the presence of the CYP3A inhibitor ketoconazole, which may lead to an overprediction of the magnitude of a xenobiotic-midazolam interaction. Because ketoconazole is no longer recommended as a clinical CYP3A inhibitor, indinavir was selected as an alternate CYP3A inhibitor to evaluate the contribution of the *N*-glucuronidation pathway to midazolam metabolism. The effects of indinavir on midazolam 1'-hydroxylation and *N*-glucuronidation were first characterized in human-derived in vitro systems. Compared to vehicle, indinavir (10 μM) inhibited midazolam 1'-hydroxylation by rCYP3A4, HLMs, and high-CYP3A activity cryopreserved human hepatocytes by ≥70%; the IC_{50} obtained with hepatocytes (2.7 μM) was within reported human unbound indinavir C_{max} (≤5 μM). Midazolam *N*-glucuronidation in hepatocytes increased in the presence of indinavir in both a concentration-dependent (1-33 μM) and time-dependent (0-4 h) manner (by up to 2.5-fold), prompting assessment in human volunteers (n=8). As predicted by these in vitro data, indinavir was a strong inhibitor of the 1'-hydroxylation pathway, decreasing the 1'-hydroxymidazolam/midazolam AUC_{0-12h} ratio by 80%. Although not statistically significant, the midazolam *N*-glucuronide/midazolam AUC_{0-12h} ratio increased by 40%, suggesting a shift to the *N*-glucuronidation pathway. The amount of midazolam *N*-glucuronide recovered in urine increased 4-fold but remained <10% of the oral midazolam dose (2.5 mg). A powered clinical study would clarify whether *N*-glucuronidation should be considered when assessing the magnitude of a xenobiotic-midazolam interaction.

DMD Fast Forward. Published on April 26, 2019 as DOI: 10.1124/dmd.119.087007
This article has not been copyedited and formatted. The final version may differ from this version.

Introduction

The cytochromes P450 (CYPs) are responsible for the oxidative metabolism of nearly 80% of clinically used drugs, with the CYP3A subfamily alone accounting for 30% of these drugs (Zanger and Schwab, 2013). Broad substrate specificity and high expression of CYP3A in both the liver and small intestine render CYP3A a major locus for drug-drug interactions (DDIs). Midazolam, a short-acting central nervous system depressant used therapeutically for sedation, anxiolysis, and amnesia, is the most widely used probe substrate for assessing CYP3A-mediated pharmacokinetic DDIs for new molecular entities (Food and Drug Administration Center for Drug Evaluation and Research, 2017a and 2017b). Midazolam is cleared primarily via 1'-hydroxylation (75%) and 4-hydroxylation (4%) by CYP3A (Heizmann and Ziegler, 1981; Dundee et al., 1984) (**Fig. 1**). Because formation of the major primary metabolite, 1'-hydroxymidazolam, is mediated solely by CYP3A, and midazolam is not a substrate for major transporters at therapeutic concentrations (Lentz et al., 2000; Tolle-Sander et al., 2003), changes in systemic exposure to midazolam almost exclusively reflect changes in CYP3A activity.

In addition to CYP3A-mediated primary metabolites, in vitro and clinical studies identified a novel primary metabolite, midazolam *N*-glucuronide, formed predominantly by UDP glucuronosyltransferase (UGT) 1A4 (Klieber et al., 2008; Zhu et al., 2008; Hyland et al., 2009). The potent CYP3A inhibitor ketoconazole nearly abolished formation of 1'-hydroxymidazolam, and in turn the corresponding 1'-*O*-glucuronide, and increased midazolam *N*-glucuronide formation approximately 6- to 8-fold in primary human hepatocytes prepared from two unrelated donors (Klieber et al., 2008). A subsequent clinical study reported midazolam *N*-glucuronide was detected in urine from six healthy male volunteers administered a single dose of 1 mg (intravenous) or 3 mg (oral) midazolam and that the *N*-glucuronidation pathway accounted for 1-2% of the midazolam dose; plasma concentrations were not measured, precluding calculation of total and renal midazolam clearance (Hyland et al., 2009). Simulations using the population-based ADME simulator Simcyp further suggested that, consistent with in vitro observations, the

DMD Fast Forward. Published on April 26, 2019 as DOI: 10.1124/dmd.119.087007
This article has not been copyedited and formatted. The final version may differ from this version.

contribution of the *N*-glucuronidation pathway increases in the presence of ketoconazole (Hyland et al., 2009). Consequently, the magnitude of a CYP3A-mediated xenobiotic-midazolam interaction could be over- or underpredicted if the *N*-glucuronidation pathway is not considered.

Due to safety concerns, oral ketoconazole is no longer recommended for clinical CYP3A-mediated DDI studies (European Medicines Agency, 2013; Food and Drug Administration, 2013 and 2016). A possible alternate CYP3A inhibitor is indinavir, which was reported to be a more potent inhibitor of testosterone 6β-hydroxylation than trifluoperazine glucuronidation using recombinant CYP3A4 and UGT1A4, respectively (IC_{50}, 0.24 vs. >100 μM) (Zhang et al., 2005; Granfors et al., 2006). Indinavir peak unbound plasma concentrations reach approximately 5 μM after oral administration of 800 mg three times daily (Boffito et al., 2003; Merck Sharp & Dohme Corp., 2016). This value is well above the IC_{50} for CYP3A4 and below that for UGT1A4, suggesting indinavir would inhibit CYP3A4 but not UGT1A4 in vivo. However, IC_{50} values recovered using recombinant enzymes are not always predictive of higher-order systems such as human liver microsomes (HLMs) and human hepatocytes.

Based on these observations, the objective of the current work was to characterize indinavir as an alternate CYP3A inhibitor using an in vitro to in vivo approach. The aims were to evaluate the effects of indinavir on midazolam 1'-hydroxylation and/or *N*-glucuronidation in (1) HLMs supplemented with cofactors for both pathways, (2) human hepatocytes, and (3) a pilot study involving human volunteers. Results provide the foundation for a powered clinical study designed to determine the contribution of *N*-glucuronidation to midazolam metabolism in vivo.

Materials and Methods

Chemicals and reagents. Midazolam and indinavir were purchased from Toronto Research Chemicals (Toronto, Canada). 1'-Hydroxymidazolam, alamethicin, magnesium chloride, saccharic acid-1,4-lactone, Tris-HCl, hecogenin acetate, β-nicotinamide adenine dinucleotide phosphate (NADPH), potassium phosphate buffer, ketoconazole, and uridine 5'-diphosphoglucuronic acid trisodium salt (UDPGA) were purchased from Sigma-Aldrich (St. Louis, MO). Midazolam 1'-*O*-glucuronide was purchased from Bioquote (York, United Kingdom). 1'-Hydroxymidazolam-d_4 was purchased from Cerilliant (Round Rock, TX). HLMs, pooled from 150 donors of mixed gender (UltraPool™), and human UGT1A4 Supersomes™ were purchased from Corning (Tewksbury, MA). All other chemicals and reagents were of analytical grade.

Midazolam *N*-glucuronide generation and isolation. Generation of midazolam *N*-glucuronide was adapted from a previously published method (Hyland et al., 2009). In brief, HLMs (0.5 mg/mL) were incubated with alamethicin (25 µg/mL), magnesium chloride (10 mM), and saccharic acid-1,4-lactone (5 mM) in Tris-HCl buffer (0.05 M, pH 7.4) on ice for 15 min to allow pore formation in the microsomal membranes. After the mixture was equilibrated to 37°C, midazolam was added to produce a final concentration of 50 µM. After an additional 5 min at 37°C, UDPGA was added to produce a final concentration of 5 mM. The final incubation volume and solvent concentration (methanol) was 100 mL and <1% (v/v), respectively. Reactions were terminated after 6 h by placing mixtures on ice and centrifuging at 3000*g* at 4°C for 20 min.

Midazolam *N*-glucuronide was extracted using a Varian BondElut C18 solid phase extraction (SPE) cartridge (Agilent, Santa Clara, CA) conditioned with 120 mL of methanol, 120 mL of acetonitrile, and 120 mL of 90/10 water/acetonitrile containing 2 mM ammonium acetate, pH 8.0. The supernatant was transferred onto the SPE cartridge then washed with 100 mL of 90/10 water/acetonitrile. Midazolam *N*-glucuronide was eluted with 120 mL of 70/30 water/acetonitrile containing 2 mM ammonium acetate, pH 8.0. The eluent was frozen on dry ice then lyophilized until a light brown powder remained. The powder was reconstituted with 90/10

DMD Fast Forward. Published on April 26, 2019 as DOI: 10.1124/dmd.119.087007
This article has not been copyedited and formatted. The final version may differ from this version.

water/acetonitrile then loaded onto a newly conditioned SPE cartridge. The eluent was washed with 3 volumes of water, eluted with 100% methanol, then lyophilized and reconstituted again in methanol-d_4 for 1H'-NMR analysis (**Supplemental Fig. S1**). The final eluent was collected, and the weight and purity were recorded.

Effects of indinavir on midazolam 1'-hydroxylation and *N*-glucuronidation in human-derived in vitro systems.

Recombinant enzymes. Recombinant CYP3A4 (rCYP3A4) or recombinant UGT1A4 (rUGT1A4) Supersomes™ (0.025 mg/mL and 0.05 mg/mL, respectively) were incubated with midazolam (5 μM) and potassium phosphate buffer (100 mM, pH 7.4) containing magnesium chloride (2 mM). Control mixtures contained 1% (v/v) dimethyl sulfoxide (DMSO) in place of ketoconazole or indinavir (10 μM). Incubation mixtures were equilibrated to 37°C, and reactions were initiated by adding UDPGA (2 mM) and/or NADPH (1 mM). After 10 min, reactions were terminated with 1 volume of ice-cold acetonitrile containing 1'-hydroxymidazolam-d_4 as internal standard. Proteins were precipitated by centrifugation (3000*g* for 10 min), and the supernatant was analyzed by LC-MS/MS for 1'-hydroxymidazolam and midazolam *N*-glucuronide (see below).

Human liver microsomes. HLMs (0.5 mg/mL) were mixed with or without alamethicin (25 μg/mL) and placed on ice. After 15 min, incubations proceeded as described for recombinant enzymes. Samples were processed and analyzed for 1'-hydroxymidazolam and midazolam *N*-glucuronide as described for recombinant enzymes.

Human hepatocytes. Single female donor cryopreserved hepatocytes (lots GGJ and XMM), characterized for CYP3A and UGT activity (6β-hydroxytestosterone and 7-hydroxycoumarin glucuronide formation, respectively), were obtained from Charles River Laboratories (Wilmington, MA). Lots were characterized as having high (lot GGJ) or low (lot XMM) CYP3A activity (152 and 10.4 pmol 6β-hydroxytestosterone/10^6 cells/min, respectively). Hepatocytes were seeded onto 96-well plates at a density of 0.5 x 10^6 viable cells/mL. Midazolam (5 μM) was added, followed by vehicle control (1% DMSO), ketoconazole (10 μM), or indinavir

DMD Fast Forward. Published on April 26, 2019 as DOI: 10.1124/dmd.119.087007
This article has not been copyedited and formatted. The final version may differ from this version.

(10 μM). Cells were incubated at 37°C, 95% relative humidity, and 5% CO_2. After 0, 0.083, 0.25, 0.5, 1, 2, or 4 h, reactions were terminated with one volume of acetonitrile containing the internal standard, 1'-hydroxymidazolam-d_4 (0.01 μM). Samples were agitated and transferred to a filter plate and filtered under positive pressure. The supernatant was analyzed for midazolam, 1'-hydroxymidazolam, and midazolam *N*-glucuronide by LC-MS/MS (see below). Area under the concentration versus time curve from 0 to 4 hours in hepatocytes ($AUC_{hep,0-4h}$) was determined using the logarithmic trapezoidal method.

Apparent IC_{50} determination. Apparent IC_{50} was determined for indinavir and the selective and potent UGT1A4 inhibitor hecogenin (Uchaipichat et al., 2006) towards midazolam 1'-hydroxylation and/or midazolam *N*-glucuronidation in HLMs (0.5 mg/ml) and the high CYP3A activity lot of cryopreserved human hepatocytes. Conditions were similar as those described above using a range of indinavir concentrations (HLMs: 0.05-300 μM; hepatocytes: 0.004-200 μM) and hecogenin (HLMs: 0.01-60 μM; hepatocytes: 0.01-30 μM); midazolam concentrations approximated the K_m for 1'-hydroxylation (4 μM) and *N*-glucuronidation (20 μM) (Klieber et al., 2008). IC_{50} estimates were recovered using untransformed data as described previously (Gufford et al., 2014) via nonlinear least-squares regression using Phoenix WinNonlin (v. 7.0; Certara USA, Inc., Princeton, NJ).

Analysis of incubations for midazolam metabolites. 1'-Hydroxymidazolam and midazolam *N*-glucuronide were quantified using a Sciex API 4000 QTRAP LC-MS/MS triple quadrupole mass spectrometer (Ontario, Canada) fitted with a Turbo ionspray interface operated in positive ion mode. A Waters Acquity UPLC system with autosampler was programmed to inject 10 μL of sample into a Varian Polaris C18-A 5 μ 100 x 3.0 mm column. Midazolam metabolites and 1'-hydroxymidazolam-d_4 were eluted with a binary gradient mixture consisting of 10 mM ammonium formate containing 1% (v/v) isopropyl alcohol and 0.1% (v/v) formic acid (A) and methanol (B) at a flow rate of 0.65 ml/min. Analytes were monitored in multiple reaction monitoring mode for the following m/z transitions: 342 → 203 (1'-hydroxymidazolam), 502 → 326 (midazolam

DMD Fast Forward. Published on April 26, 2019 as DOI: 10.1124/dmd.119.087007
This article has not been copyedited and formatted. The final version may differ from this version.

N-glucuronide), and 346 → 203 (1'-hydroxymidazolam-d_4). Metabolite concentrations were determined by interpolation from a linear standard curve with a dynamic range of 0.0005-5 μM. Quality controls (QCs), prepared at three different concentrations and stored with study samples, were analyzed with each batch of samples against separately prepared calibration standards. Acceptance criteria were that no more than one-third of the total QC results and no more than one-half of the results from each concentration deviated from the nominal concentration by more than 15%. Inter- and intraday variability in the QCs were less than 10%.

Clinical Study

A prospective, randomized, open-label crossover study was conducted at the University of North Carolina Clinical and Translational Research Center (CTRC). The study protocol and consent form were reviewed and approved by the Office of Human Research Ethics/Biomedical Institutional Review Board and the CTRC Oversight Committee at the University of North Carolina at Chapel Hill. Written informed consent and Health Insurance Portability and Accountability Act authorization were obtained from each volunteer prior to participation.

Participants. Healthy, HIV-seronegative volunteers (four men, five women) were enrolled. Eight participants were deemed sufficient for this pilot study. One woman withdrew from the study prior to drug administration due to intolerance to study procedures. The men and women ranged in age from 27 to 62 years and 31 to 51 years, respectively. Participants were self-identified as Caucasian (two men, two women), African American (one man, one woman), Hispanic (one man), and Asian (one woman).

Before enrollment, each participant underwent a medical history, physical examination, liver function tests, complete blood count, and HIV testing. Each woman of child-bearing age underwent a serum pregnancy test. None of the participants were taking known modulators of CYP3A or UGT activity. Participants were asked to abstain from all fruit juices one week before and during the study and from alcohol and caffeinated beverages the evening before each study day.

Procedures. Block randomization, stratified by sex, was used to assign participants to each of two phases: midazolam alone (control) or midazolam + indinavir (treatment). A minimum of one week separated the two phases (**Fig. 2**). Vital signs (blood pressure, temperature, pulse, respirations) and oxygen saturation were obtained at the initiation of each phase and monitored periodically thereafter; the women underwent an additional urine pregnancy test before administration of the first dose of indinavir. Participants were administered water (250 mL) or 800 mg of indinavir (Crixivan®, Merck & Co., Inc., Whitehouse Station, NJ) orally with water (250 mL) on the evening of Day 1; a snack was administered immediately thereafter to minimize gastrointestinal upset, and participants were monitored the following hour for side effects prior to discharge. After an overnight fast, participants returned to the CTRC the morning of Day 2 and were administered water or indinavir (800 mg) with water and a snack; indinavir dosing was repeated every 6 h x 2 doses (3 doses total). One hour after the first administration of water alone or with indinavir on the morning of Day 2, participants were administered 2.5 mg of midazolam syrup (Ranbaxy Pharmaceuticals, Inc., Jacksonville, FL) with water (250 mL). Blood (7 mL) was collected from an arm vein via an indwelling intravenous catheter pre-midazolam administration and at 0.5, 1, 1.5, 2, 3, 4, 5, 6, 8, 10, and 12 h post-midazolam administration. Plasma was separated from blood cells via centrifugation within 1 h of collection and was stored at -80°C pending analysis for midazolam and metabolites by LC-MS/MS. Urine was collected from 0-6 and 6-12 h. Plasma and urine were processed, stored at -80 °C, and analyzed within 6 months of collection.

Analysis of plasma and urine for midazolam and metabolites. Plasma and urine were analyzed for midazolam, 1'-hydroxymidazolam, midazolam 1'-*O*-glucuronide, and midazolam *N*-glucuronide by LC-MS/MS using a similar method as described for the in vitro studies. In brief, 150 µL acetonitrile containing 1'-hydroxymidazolam-d_4 were added to 50 µL of plasma or urine, centrifuged (3000 x g), and the supernatant (10 µL) was injected into the LC-MS/MS system. Additional m/z transitions included 326 → 291 (midazolam) and 518 → 324 (midazolam 1'-*O*-

DMD Fast Forward. Published on April 26, 2019 as DOI: 10.1124/dmd.119.087007
This article has not been copyedited and formatted. The final version may differ from this version.

glucuronide). The dynamic range for midazolam and midazolam 1'-*O*-glucuronide was 0.0005-5 μM and 0.001-5 μM, respectively. QCs were prepared and interpreted as described above.

Pharmacokinetic analysis. The pharmacokinetics of midazolam and metabolites were determined by noncompartmental methods using Phoenix® WinNonlin® (v. 7.0). Terminal elimination rate constant (λ_z) was estimated by linear regression of the terminal portion of the log-transformed concentration versus time curve using at least the last three data points. Terminal half-life ($t_{1/2}$) was calculated as $\ln(2)/\lambda_z$. The maximum concentration (C_{max}) and time to reach C_{max} (t_{max}) were obtained directly from the concentration-time profile. The AUC from 0 to 12 h ($AUC_{0\text{-}12h}$) was determined using the trapezoidal method with linear up/log down interpolation. The percentage of the total amount recovered in urine was calculated by dividing the amount of analyte measured ($A_{e,0\text{-}12h}$) by total drug-related material measured over the 12 h collection period. Renal clearance (Cl_R) was calculated as $A_{e,0\text{-}12h}/AUC_{0\text{-}12h}$.

Statistical analysis

A Student's t test and one-way ANOVA were used to compare two groups and three groups, respectively, regarding the formation of 1'-hydroxymidazolam or midazolam *N*-glucuronide in the various in vitro systems using GraphPad Prism 5.0 (GraphPad Software, La Jolla, CA). Pharmacokinetic outcomes were compared between control and indinavir treatment using a paired two-tailed Student's *t*-test within SAS (v. 9.4, SAS Institute Inc,, Cary, NC); with the exception of t_{max}, outcomes were log-transformed prior to the analysis. *P*-values < 0.05 were considered significant.

DMD Fast Forward. Published on April 26, 2019 as DOI: 10.1124/dmd.119.087007
This article has not been copyedited and formatted. The final version may differ from this version.

Results

Indinavir inhibits midazolam 1'-hydroxylation but not *N*-glucuronidation in human-derived in vitro systems. Midazolam 1'-hydroxylation and *N*-glucuronidation were evaluated in the absence and presence of indinavir, the positive control CYP3A inhibitor ketoconazole, and the UGT1A4 inhibitor hecogenin. *Recombinant enzymes.* Compared to control incubations containing NADPH (+/- UDPGA), both ketoconazole and indinavir inhibited midazolam 1'-hydroxylation by rCYP3A4, by >95% (P<0.001) (**Fig. 3A**); compared to control incubations containing UDPGA (+/- NADPH), ketoconazole had no effect, and indinavir had minor effects (<25% inhibition) on midazolam *N*-glucuronide formation by rUGT1A4 (P>0.17) (**Fig. 3B**). *Human liver microsomes.* Compared to control incubations containing NADPH (+UDPGA), in the absence and presence of alamethicin, both indinavir and ketoconazole inhibited the formation of 1'-hydroxymidazolam, by 99%, (P<0.001) (**Fig. 4A**); compared to control incubations containing UDPGA (+/- NADPH), ketoconazole increased midazolam *N*-glucuronide formation (by ~40%) (P<0.05) and indinavir had no effect (**Fig. 4B**). The presence of alamethicin inhibited 1'-hydroxymidazolam formation (by 25%) (P<0.001) (**Fig. 4A**) but did not affect the magnitude of change in formation of both 1'-hydroxymidazolam and midazolam *N*-glucuronide (**Fig. 4B**). *Cryopreserved human hepatocytes.* In the absence of CYP3A inhibitors, 1'-hydroxymidazolam formation in the high CYP3A activity lot increased up to 2 h then decreased slightly to 4 h, whereas in the low CYP3A activity lot, formation increased throughout the 4-h incubation period (**Fig. 5A and C**). Midazolam *N*-glucuronide formation increased throughout the 4 h incubation period in both the high and low CYP3A activity lots (**Fig. 5B and D**). Ketoconazole and indinavir inhibited the time-averaged formation of 1'-hydroxymidazolam, as assessed by the $AUC_{hep,0-4h}$, in both the high CYP3A activity lot (by 93 and 68 %, respectively) (P<0.001) and low CYP3A activity lot (by 85 and 23%, respectively) (P<0.01 and P>0.08, respectively) (**Fig. 5A and C**). Ketoconazole increased midazolam *N*-glucuronide $AUC_{hep,0-4h}$ in both the high and low CYP3A activity lots (by

DMD Fast Forward. Published on April 26, 2019 as DOI: 10.1124/dmd.119.087007
This article has not been copyedited and formatted. The final version may differ from this version.

8.5- and 1.9-fold, respectively), and indinavir increased midazolam *N*-glucuronide $AUC_{hep,0-4h}$ in the high-activity lot (by up to 2.5-fold) (**Fig. 5B and D**).

The apparent IC_{50} values of indinavir indicate selectivity towards midazolam 1'-hydroxylation. Indinavir was a potent inhibitor of midazolam 1'-hydroxylation in cryopreserved human hepatocytes, with an IC_{50} of 2.7 μM (**Fig. 6A**); regarding midazolam *N*-glucuronidation, indinavir had no effect (up to 0.15 μM), increased (1-33 μM), or inhibited activity by 58% at 200 μM (**Fig. 6C**). Hecogenin inhibited midazolam 1'-hydroxylation by ~30% (0.004-30 μM) (**Fig. 6B**) and was a potent inhibitor of midazolam *N*-glucuronidation, with an IC_{50} of 0.12 μM (**Fig. 6D**). Indinavir was a much weaker inhibitor of midazolam *N*-glucuronidation in HLMs (IC_{50}, 79 μM) than hecogenin (IC_{50}, 2.3 μM (**Fig. 7A and 7B**).

Indinavir is a strong inhibitor of midazolam 1'-hydroxylation in healthy volunteers. Eight subjects were randomized to receive oral midazolam (2.5 mg) alone or 1 h after the morning dose of oral indinavir on Day 2 (800 mg) (**Fig. 2**). Relative to midazolam alone, geometric mean plasma concentrations of midazolam were higher upon co-administration with indinavir (**Fig. 8A**); midazolam *N*-glucuronide concentrations also were higher (**Fig. 8B**). Midazolam and midazolam *N*-glucuronide systemic exposure (AUC_{0-12h}) increased by 9.7- and 14-fold, respectively (**Table 1**). The AUC_{0-12h} for both 1'-hydroxymidazolam and midazolam 1'-*O*-glucuronide decreased by ~55% in the presence of indinavir (**Figs. 8C and 8D, Table 1**). Metabolite ratios, calculated as the AUC_{0-12h} ratio of a metabolite to midazolam, decreased by ~95% for 1'-hydroxymidazolam and midazolam 1'-*O*-glucuronide and remained unchanged for midazolam *N*-glucuronide (**Table 1**). Midazolam oral clearance decreased by 94%, and the half-life doubled, in the presence of indinavir. The half-life for midazolam *N*-glucuronide, 1'-hydroxymidazolam, and midazolam 1'-*O*-glucuronide in the presence of indinavir could not be determined accurately due to an insufficient collection period.

All analytes were quantifiable in urine except for 1'-hydroxymidazolam in the presence of indinavir (**Table 2**). Midazolam 1'-*O*-glucuronide was the most abundant analyte recovered in

urine, accounting for 99% and 89% of total midazolam-related material (midazolam + metabolites) recovered, respectively, in the absence and presence of indinavir. Total urinary recovery of midazolam-related material decreased by 47% in the presence of indinavir. Indinavir decreased renal clearance of midazolam and midazolam *N*-glucuronide by 70-80% and had no effect on that of midazolam 1'-*O*-glucuronide (**Table 2**).

DMD Fast Forward. Published on April 26, 2019 as DOI: 10.1124/dmd.119.087007
This article has not been copyedited and formatted. The final version may differ from this version.

Discussion

Midazolam remains the gold standard index CYP3A substrate for assessing the modulatory effects of new molecular entities and other xenobiotics, including botanical and other natural products, for both in vitro and clinical studies (European Medicines Agency, 2012; Food and Drug Administration, 2017a). Primary clearance pathways of midazolam include CYP3A-mediated 1'- and 4-hydroxylation and UGT1A4-mediated *N*-glucuronidation, the latter of which has not been extensively characterized in vivo. Simulated pharmacokinetic studies indicated that the contribution of the *N*-glucuronidation pathway increased in the presence of ketoconazole, complicating assessment of the CYP3A-mediated DDI (Hyland et al., 2009). However, such simulations require verification to confirm or refute these observations. Because ketoconazole is no longer a recommended CYP3A inhibitor for clinical DDI studies, indinavir was selected as an alternate CYP3A inhibitor. The inhibition of indinavir towards midazolam metabolism was first characterized using human-derived in vitro systems before evaluating in healthy human volunteers.

The selective UGT1A4 inhibitor hecogenin (Uchaipichat et al., 2006) inhibited midazolam *N*-glucuronide formation in a concentration-dependent manner in both cryopreserved human hepatocytes (IC_{50}, 0.12 μM) and HLMs (IC_{50}, 2.3 μM) (**Fig. 6D and 7B**), confirming a major role for UGT1A4 in the *N*-glucuronidation of midazolam (Klieber et al., 2008). In the current work, indinavir at 10 μM nearly ablated rCYP3A4 activity but not rUGT1A4 activity (**Fig. 3**), consistent with previous reports (Zhang et al., 2005; Granfors et al., 2006). The high IC_{50} value (79 μM) for indinavir towards midazolam *N*-glucuronidation in HLMs (**Fig. 7A**), combined with the lack of inhibition by indinavir (up to 33 μM) in hepatocytes (**Fig. 6C**), further supported indinavir as a selective CYP3A inhibitor and a weak inhibitor of midazolam *N*-glucuronidation. Consistent with a previous report involving primary human hepatocytes (Klieber et al., 2008), ketoconazole increased midazolam *N*-glucuronidation in cryopreserved human hepatocytes (**Fig. 5B**). Indinavir also increased midazolam *N*-glucuronidation, albeit the effects were less pronounced (**Fig. 5D**

and 6C), which may due to indinavir being a less potent inhibitor of CYP3A activity compared to ketoconazole (IC_{50}, 0.24 versus 0.05 μM) (Patki et al., 2003; Granfors et al., 2006). Collectively, these in vitro data suggested indinavir as a suitable alternate selective CYP3A inhibitor to determine if midazolam metabolism shifts to the *N*-glucuronidation pathway in the presence of CYP3A inhibition in heathy human volunteers.

In the present study, indinavir increased geometric mean midazolam *N*-glucuronide $AUC_{0\text{-}12h}$ by 13.5-fold, whereas 1'-hydroxymidazolam $AUC_{0\text{-}12h}$ decreased by 50%, in healthy volunteers. The metabolic ratios 1'-hydroxymidazolam/midazolam and midazolam 1'-*O*-glucuronide/midazolam both decreased by 95%, consistent with the in vitro data showing indinavir as a strong inhibitor of CYP3A activity. Although not statistically significant, the metabolic ratio of midazolam *N*-glucuronide/midazolam increased by 40%. Consistent with plasma data, midazolam *N*-glucuronide represented ~1% and 8% of the total midazolam-related material recovered in urine in the absence and presence of indinavir, respectively. These results suggested a shift to the *N*-glucuronidation pathway by indinavir, as predicted by human hepatocytes.

Midazolam is recovered in urine predominately as the 1'-*O*-glucuronide (Heizmann and Ziegler, 1981) and represented 99% and 89% of midazolam-related material in the absence and presence of indinavir, respectively (**Table 2**). Compared to the absence of indinavir, the renal clearance of the 1'-*O*-glucuronide was unchanged in the presence of indinavir, whereas that for the *N*-glucuronide decreased by ~70%. Assuming negligible plasma protein binding and an average glomerular filtration rate of 6 L/h (Grewal and Blake, 2005), both glucuronides undergo net renal secretion, which represents roughly 50% of total renal clearance. These observations indicate that indinavir inhibited net secretory clearance of the *N*-glucuronide but not the 1'-*O*-glucuronide, suggesting different transport mechanisms between the two glucuronides that are as yet not known. Despite the decrease in the renal clearance of the *N*-glucuronide, the amount recovered in the urine increased, further suggesting a shift to the *N*-glucuronidation pathway in the presence of indinavir.

There are limitations to the current work. First, only two lots of hepatocytes were used to determine the effects of indinavir on midazolam *N*-glucuronidation. However, results with the more potent CYP3A inhibitor ketoconazole were consistent with a previous report involving 18 lots of primary human hepatocytes (Klieber et al., 2008). Second, the clinical study was not powered to make definitive conclusions about the contribution of the *N*-glucuronidation pathway to midazolam metabolism. The contribution of this alternate pathway could be clarified by conducting a powered clinical study comparing the effects of a dual CYP3A/UGT1A4 inhibitor, such as ritonavir (Zhang et al., 2005), to the effects of a selective CYP3A inhibitor, such as indinavir, on the disposition of midazolam and metabolites.

In summary, the suitability of indinavir as an alternate and selective CYP3A inhibitor to ketoconazole to assess the contribution of the *N*-glucuronidation pathway to midazolam metabolism was characterized in established human-derived in vitro systems and in eight healthy volunteers. Although the increase in the amount of midazolam *N*-glucuronide recovered in urine remained low in the presence of indinavir (<10%), the substantive decrease in *N*-glucuronide renal clearance may have masked the true contribution of the *N*-glucuronidation pathway to midazolam metabolism. A powered clinical study is needed to determine definitively whether *N*-glucuronidation should be considered when assessing the magnitude of a CYP3A-mediated xenobiotic-drug interaction involving midazolam as the probe substrate.

Acknowledgements

The authors thank the staff at the University of North Carolina Clinical and Translational Research Center for their help with the clinical study. The authors thank Dr. Matthew A, Cerny (Pfizer Inc., formerly at Boerhinger-Ingelheim) for his help with the bioanalytical aspects of the work and Dr. Zuping Xia (Department of Pharmaceutics, Washington State University) for his help with the interpretation of the HNMR spectrum. M.F.P. dedicates this article to Dr. David P. Paine.

Authorship Contributions

Participated in research design: Leonowens, Frederick, Scarlett, Fisher, and Paine

Conducted experiments: Leonowens, Frederick, and Scarlett

Contributed new reagents or analytic tools: Frederick and Fisher

Performed data analysis: Tian, Leonowens, González-Pérez, Cox, and Frederick

Wrote or contributed to the writing of the manuscript: Tian, Leonowens, González-Pérez, Cox, and Paine

REFERENCES

Boffito M, Back DJ, Blaschke TF, Rowland M, Bertz RJ, Gerber JG, and Miller V (2003) Protein binding in antiretroviral therapies. *AIDS Res Hum Retroviruses* **19:**825-835.

Dundee JW, Halliday NJ, Harper KW, and Brogden RN (1984) Midazolam. A review of its pharmacological properties and therapeutic use. *Drugs* **28:**519-543.

European Medicines Agency (2012) *Guideline on the investigation of drug interactions*, European Medicines Agency, London

European Medicines Agency (2013) European Medicines Agency recommends suspension of marketing authorisations for oral ketoconazole. https://www.ema.europa.eu/en/news/european-medicines-agency-recommends-suspension-marketing-authorisations-oral-ketoconazole. Accessed on April 12, 2019.

Food and Drug Administration (2013) FDA Drug Safety Communication: FDA limits usage of Nizoral (ketoconazole) oral tablets due to potentially fatal liver injury and risk of drug interactions and adrenal gland problems. https://www.fda.gov/drugs/drugsafety/ucm362415.htm. Accessed on April 12, 2019.

Food and Drug Administration (2016) FDA Drug Safety Communication: FDA warns that prescribing of Nizoral (ketoconazole) oral tablets for unapproved uses including skin and nail infections continues; linked to patient death. https://www.fda.gov/Drugs/DrugSafety/ucm500597.htm. Accessed on April 12, 2019.

Food and Drug Administration Center for Drug Evaluation and Research (2017a) *Drug Interaction Studies —Study Design, Data Analysis, Implications for Dosing, and Labeling. Recommendations*, U.S. Food and Drug Administration, Silver Spring, MD.

Food and Drug Administration Center for Drug Evaluation and Research (2017b) *In Vitro Metabolism and Transporter-Mediated Drug-Drug Interaction Studies. Guidance for Industry*, U.S. Food and Drug Administration, Silver Spring, MD.

Granfors MT, Wang JS, Kajosaari LI, Laitila J, Neuvonen PJ, and Backman JT (2006) Differential inhibition of cytochrome P450 3A4, 3A5 and 3A7 by five human immunodeficiency virus (HIV) protease inhibitors in vitro. *Basic & clinical pharmacology & toxicology* **98:**79-85.

Grewal GS and Blake GM (2005) Reference data for 51Cr-EDTA measurements of the glomerular filtration rate derived from live kidney donors. *Nucl Med Commun* **26:**61-65.

Gufford BT, Chen G, Lazarus P, Graf TN, Oberlies NH, and Paine MF (2014) Identification of diet-derived constituents as potent inhibitors of intestinal glucuronidation. *Drug metabolism and disposition: the biological fate of chemicals* **42:**1675-1683.

Heizmann P and Ziegler WH (1981) Excretion and metabolism of 14C-midazolam in humans following oral dosing. *Arzneimittel-Forschung* **31:**2220-2223.

Hyland R, Osborne T, Payne A, Kempshall S, Logan YR, Ezzeddine K, and Jones B (2009) In vitro and in vivo glucuronidation of midazolam in humans. *British journal of clinical pharmacology* **67:**445-454.

Klieber S, Hugla S, Ngo R, Arabeyre-Fabre C, Meunier V, Sadoun F, Fedeli O, Rival M, Bourrie M, Guillou F, Maurel P, and Fabre G (2008) Contribution of the N-glucuronidation pathway to the overall in vitro metabolic clearance of midazolam in humans. *Drug metabolism and disposition: the biological fate of chemicals* **36:**851-862.

Lentz KA, Polli JW, Wring SA, Humphreys JE, and Polli JE (2000) Influence of passive permeability on apparent P-glycoprotein kinetics. *Pharmaceutical research* **17:**1456-1460.

Merck Sharp & Dohme Corp. (2016) [Crixivan(R) (Indinavir Sulfate) Capsules [package insert], Whitehouse Station, NJ.

Patki KC, Von Moltke LL, and Greenblatt DJ (2003) In vitro metabolism of midazolam, triazolam, nifedipine, and testosterone by human liver microsomes and recombinant cytochromes p450: role of cyp3a4 and cyp3a5. *Drug metabolism and disposition: the biological fate of chemicals* **31:**938-944.

Tolle-Sander S, Rautio J, Wring S, Polli JW, and Polli JE (2003) Midazolam exhibits characteristics of a highly permeable P-glycoprotein substrate. *Pharmaceutical research* **20:**757-764.

Uchaipichat V, Mackenzie PI, Elliot DJ, and Miners JO (2006) Selectivity of substrate (trifluoperazine) and inhibitor (amitriptyline, androsterone, canrenoic acid, hecogenin, phenylbutazone, quinidine, quinine, and sulfinpyrazone) "probes" for human udp-glucuronosyltransferases. *Drug metabolism and disposition: the biological fate of chemicals* **34:**449-456.

Zanger UM and Schwab M (2013) Cytochrome P450 enzymes in drug metabolism: regulation of gene expression, enzyme activities, and impact of genetic variation. *Pharmacology & therapeutics* **138:**103-141.

Zhang D, Chando TJ, Everett DW, Patten CJ, Dehal SS, and Humphreys WG (2005) In vitro inhibition of UDP glucuronosyltransferases by atazanavir and other HIV protease inhibitors and the relationship of this property to in vivo bilirubin glucuronidation. *Drug metabolism and disposition: the biological fate of chemicals* **33:**1729-1739.

Zhu B, Bush D, Doss GA, Vincent S, Franklin RB, and Xu S (2008) Characterization of 1'-hydroxymidazolam glucuronidation in human liver microsomes. *Drug metabolism and disposition: the biological fate of chemicals* **36:**331-338.

Footnotes

a. This work was supported in part by the National Institutes of Health (NIH) National Institute of General Medical Sciences [Grant R01 GM077482], the NIH National Center for Complimentary and Integrative Health (Grant U54 AT008909), and the NIH National Center for Research Resources/National Center for Advancing Translational Sciences [Grant UL1 RR025747 (now UL1 TR002489). The content is solely the responsibility of the authors and does not necessarily represent the official views of the NIH.

b. Reprint requests: Mary F. Paine, RPh, PhD

PBS 341, PO Box 1495

College of Pharmacy and Pharmaceutical Sciences

Washington State University

Spokane, WA 99210-1495

Telephone: 509-358-7759

FAX: 509-368-6673

E-mail: mary.paine@wsu.edu

[†]Deceased.

[1]Current Address: Nuventra Pharma Sciences, Durham, NC

[2]Current Address: Providence Medical Research Center, Providence Health Care, Spokane, WA

[3]Current Address: Office of the Dean of the Graduate School, Princeton University, Princeton, NJ

[4]Current Address: Bristol-Myers Squibb, Wallingford, CT

Legends for Figures

Figure 1. Midazolam metabolic pathways.

Figure 2. Clinical study design. Drug administration schedule: Day 1 (PM) indinavir (IDV); Day 2, IDV (AM), followed by a single dose of midazolam (MDZ) marking the 0 h time point and an additional IDV dose at 5 h. Post midazolam administration, blood and urine were collected at 0.5, 1, 1.5, 2, 3, 4, 5, 6, 8, 10, and 12 h or 0-6 and 6-12 intervals, respectively.

Figure 3. Inhibition of midazolam 1'-hydroxylation (A) and *N*-glucuronidation (B) by ketoconazole (KTZ) and indinavir (IDV) using recombinant CYP3A4 (A) and UGT1A4 (B). Reactions were initiated with NADPH alone (+NADPH/-UDPGA), UDPGA alone (-NADPH/+UDPGA), or with both NADPH and UDPGA (+NADPH/+UDGPA). Bars and error bars denote means and SDs, respectively, of three technical replicates.

Figure 4. Effects of ketoconazole (KTZ) and indinavir (IDV) on midazolam 1'-hydroxylation (A) and *N*-glucuronidation (B) in HLMs. Incubation mixtures were pre-treated without alamethicin (-Alamethicin) or with alamethicin (+Alamethicin) before initiating the reactions with UDPGA alone (-NADPH/+UDPGA), or with both NADPH and UDPGA (+NADPH/+UDGPA). Bars and error bars denote means and SDs, respectively, of three technical replicates.

Figure 5. Time-dependent effects of ketoconazole (A and B) and indinavir (C and D) on midazolam 1'-hydroxylation (A and C) or *N*-glucuronidation (B and D) in cryopreserved human hepatocytes. Symbols and error bars denote means and SDs, respectively, of three technical replicates. [I], inhibitor.

Figure 6. Concentration-dependent effects of indinavir and hecogenin on midazolam 1'-hydroxylation (A and B) and *N*-glucuronidation (C and D) in cryopreserved human hepatocytes. Symbols represent three technical replicates. Curves denote nonlinear least-squares regression of the data using Phoenix WinNonlin (v. 7.0).

Figure 7. Concentration-dependent inhibition of midazolam *N*-glucuronidation by indinavir (A) and hecogenin (B) in HLMs. Symbols represent three technical replicates. Curves denote nonlinear least-squares regression of the data using Phoenix WinNonlin (v. 7.0).

Figure 8. Plasma concentration-time profiles for midazolam (A), midazolam *N*-glucuronide (B), 1'-hydroxymidazolam (C), and midazolam 1'-*O*-glucuronide (D) in the absence (midazolam only, open symbols) or presence (midazolam + indinavir, solid symbols) of indinavir. Symbols and error bars denote geometric means and upper and lower limits of the 90% confidence interval, respectively.

DMD Fast Forward. Published on April 26, 2019 as DOI: 10.1124/dmd.119.087007
This article has not been copyedited and formatted. The final version may differ from this version.

Table 1. Plasma pharmacokinetics of midazolam and metabolites (n=8 subjects).

	Geometric mean [90% confidence interval]		
	Control	Treatment	Treatment/Control
Midazolam			
$AUC_{0\text{-}12h}$ (nM·h)	63.5 [51.3-78.5]	614 [499-756]*	9.7 [7.6-12.3]
C_{max} (nM)	23.2 [18.9-28.5]	128 [108-153]*	5.5 [4.3-7.1]
$t_{1/2}$ (h)	2.96 [2.22-3.95]	5.72 [4.75-6.89]*	NC
t_{max} (h)[a]	1.0 [0.5-1.0]	1.0 [0.5-2.0]	NC
Cl/F (L/h)	113 [90.4-141]	6.69 [4.42-10.1]*	0.06 [0.04-0.09]
Midazolam *N*-glucuronide			
$AUC_{0\text{-}12h}$ (nM·h)	4.02 [1. 57-10.3]	54.4 [42.2-70.3]*	13.5 [5.8-32]
Metabolic ratio[b]	0.063 [0.027-0.15]	0.088 [0.072-0.11]	1.40 [0.72-2.73]
C_{max} (nM)	1.31 [0.89-1.92]	6.81 [5.18-8.94]*	5.2 [4.0-6.8]
$t_{1/2}$ (h)	5.35 [3.09-9.26]	NA	NC
t_{max} (h)[a]	4.0 [3.0-6.0]	6.0 [4.0-10.0]*	NC
1'-Hydroxymidazolam			
$AUC_{0\text{-}12h}$ (nM·h)	29.3 [22.0-39.0]	13.5 [11.2-16.1]*	0.46 [0.31-0.69]
Metabolic ratio[b]	0.46 [0.38-0.55]	0.022 [0.016-0.030]*	0.05 [0.03-0.07]
C_{max} (nM)	11.1 [8.94-13.7]	2.31 [1.90-2.81]*	0.21 [0.14-0.30]
$t_{1/2}$ (h)	2.05 [1.44-2.92]	NA	NC
t_{max} (h)[a]	1.0 [0.5-1.0]	5.0 [2.0-6.0]*	NC
Midazolam 1'-*O*-glucuronide			
$AUC_{0\text{-}12h}$ (nM·h)	415 [362-475]	180 [155-210]*	0.43 [0.33-0.57]
Metabolic ratio[b]	6.53 [5.69-7.53]	0.29 [0.21-0.41]*	0.045 [0.032-0.064]
C_{max} (nM)	163 [146-181]	26.5 [21.2-33.0]*	0.16 [0.12-0.21]

DMD Fast Forward. Published on April 26, 2019 as DOI: 10.1124/dmd.119.087007
This article has not been copyedited and formatted. The final version may differ from this version.

$t_{1/2}$ (h)	3.58 [2.88-4.43]	NA	NC
t_{max} (h)[a]	1.0 [0.5-1.0]	5.0 [2.0-6.0]*	NC

$AUC_{0\text{-}12h}$, area under the plasma concentration versus time curve from 0-12 h; C_{max}, maximum plasma concentration; $t_{½}$, terminal half-life; t_{max}, time to reach C_{max}; Cl/F, apparent oral clearance. NA, not applicable; NC, not calculable.

[a] Denote median [range].

[b] Calculated by dividing the $AUC_{0\text{-}12h}$ of metabolite by the $AUC_{0\text{-}12h}$ of midazolam.

*P < 0.05 compared to control group.

DMD Fast Forward. Published on April 26, 2019 as DOI: 10.1124/dmd.119.087007
This article has not been copyedited and formatted. The final version may differ from this version.

Table 2. Urinary excretion of midazolam and metabolites (n=8 subjects).

	Geometric mean [90% confidence interval]		
	Control	Treatment	Treatment/Control
Midazolam			
$A_{e,0\text{-}12h}$ (nmol)	7.7 [5.9-10]	15 [11-21]*	2 [1.3-2.9]
% of total amount recovered	0.14 [0.11-0.18]	0.53 [0.34-0.81]*	NA
Cl_R (L/h)	0.12 [0.10-0.15]	0.02 [0.02-0.04]*	0.2 [0.13-0.31]
Midazolam *N*-glucuronide			
$A_{e,0\text{-}12h}$ (nmol)	53 [43-66]	230 [130-400]*	4.3 [2.1-8.9]
% of total amount recovered	0.98 [0.78-1.2]	8.1 [4.6-14]*	NA
Cl_R (L/h)	13 [6.2-28]	4.3 [2.1-8.7]*	0.32 [0.14-0.72]
1'-Hydroxymidazolam			
$A_{e,0\text{-}12h}$ (nmol)	5.7 [4.7-7.0]	NQ	NA
% of total amount recovered	0.11 [0.09-0.13]	NQ	NA
Cl_R (L/h)	0.2 [0.14-0.27]	NQ	NA
Midazolam 1'-*O*-glucuronide			
$A_{e,0\text{-}12h}$ (nmol)	5400 [5100-5700]	2600 [2100-3100]*	0.48 [0.39-0.59]
% of total amount recovered	99 [98-99]	89 [86-93]*	NA
Cl_R (L/h)	13 [11-15]	14 [12-17]	1.1 [0.82-1.5]
Total amount recovered (nmol)	5400 [5200-5700]	2856 [2400-3400]	0.53 [0.43-0.64]

$A_{e,0\text{-}12h}$, amount recovered in 12 h post-dose; Cl_R, renal clearance; NQ, not quantifiable; NA, not applicable

*P < 0.05 compared to control group.

DMD Fast Forward. Published on April 26, 2019 as DOI: 10.1124/dmd.119.087007
This article has not been copyedited and formatted. The final version may differ from this version.

Figure 1.

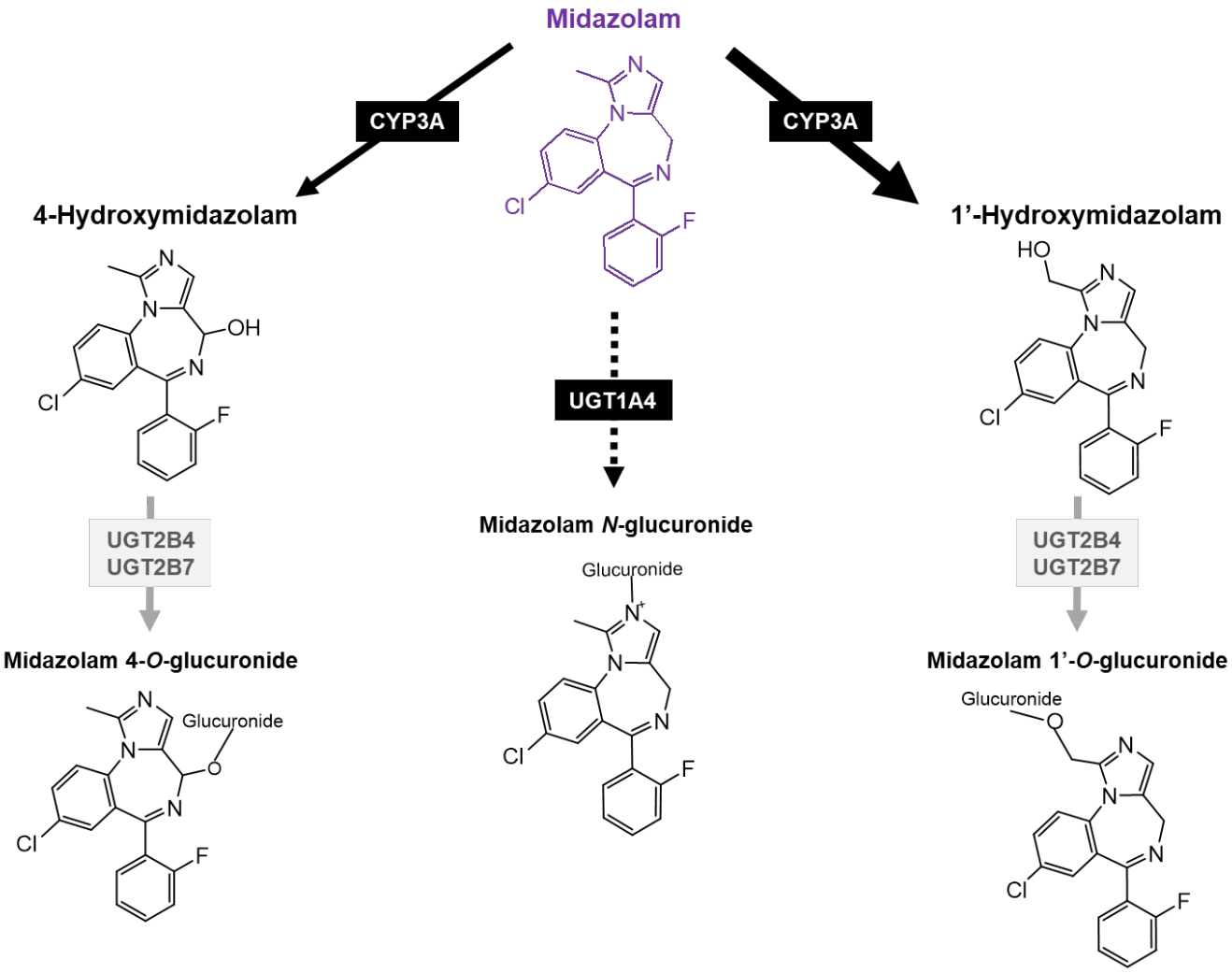

DMD Fast Forward. Published on April 26, 2019 as DOI: 10.1124/dmd.119.087007
This article has not been copyedited and formatted. The final version may differ from this version.

Figure 2.

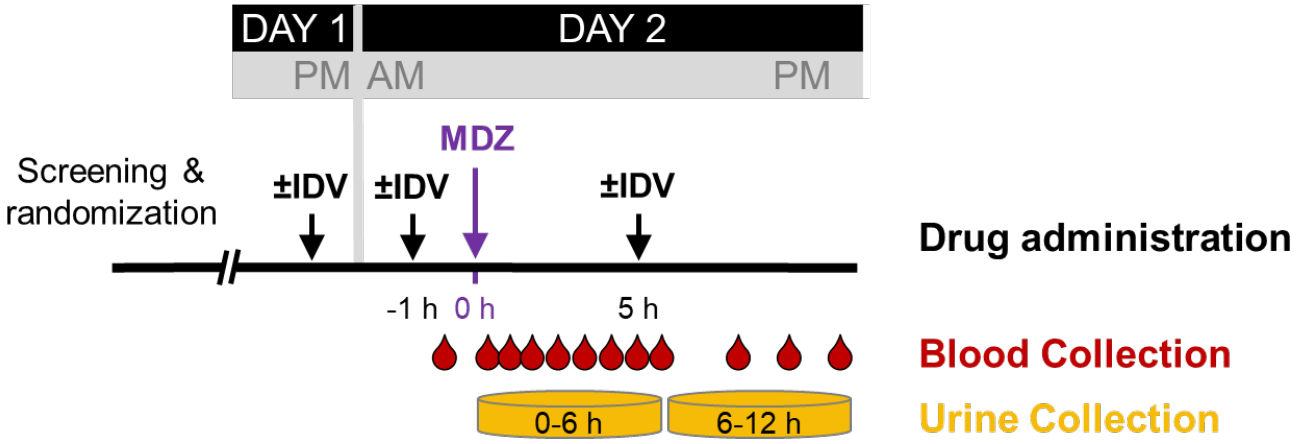

DMD Fast Forward. Published on April 26, 2019 as DOI: 10.1124/dmd.119.087007
This article has not been copyedited and formatted. The final version may differ from this version.

Figure 3.

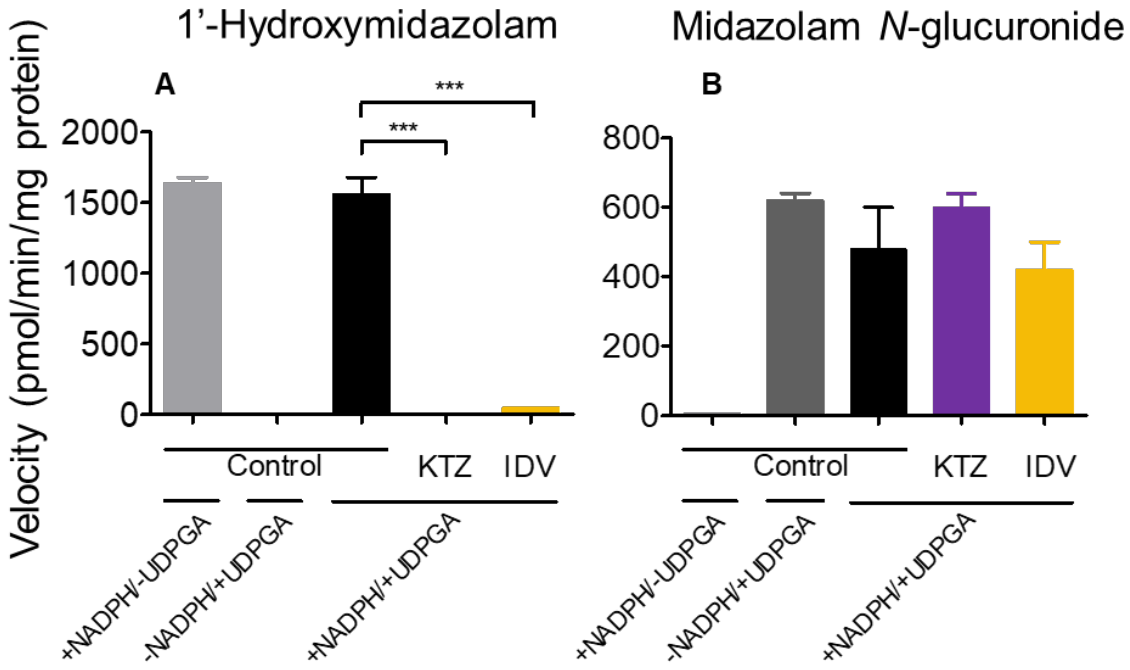

DMD Fast Forward. Published on April 26, 2019 as DOI: 10.1124/dmd.119.087007
This article has not been copyedited and formatted. The final version may differ from this version.

Figure 4.

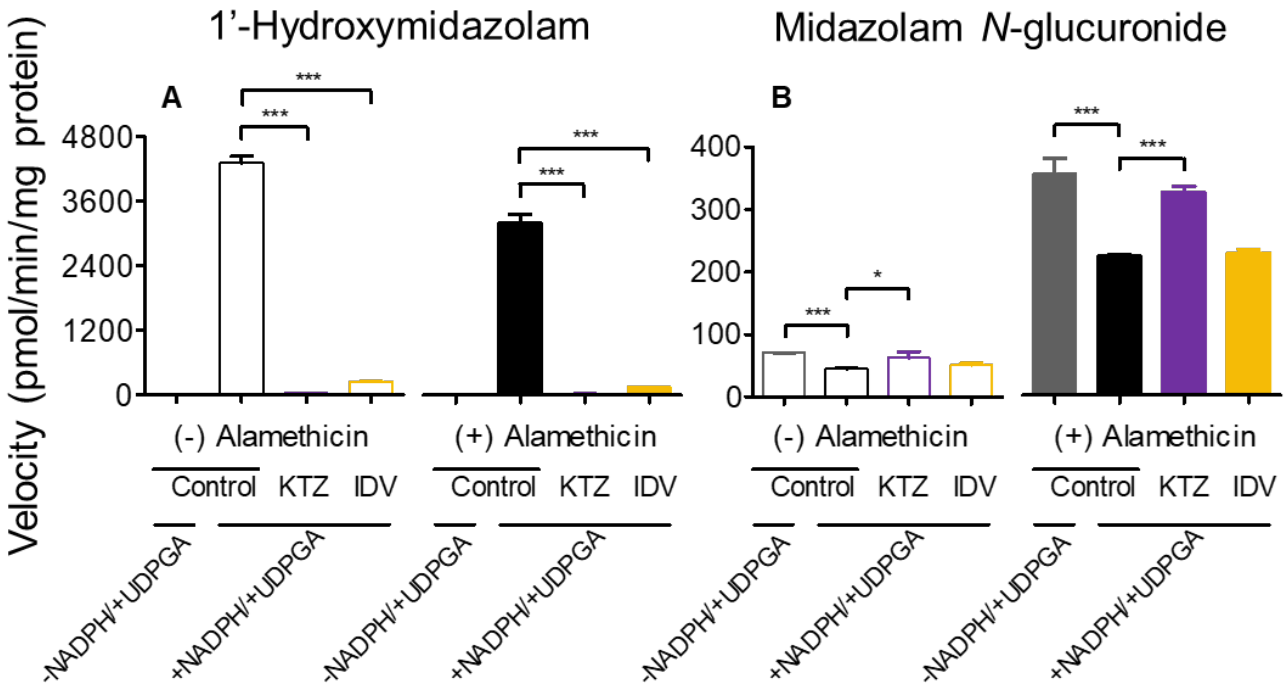

DMD Fast Forward. Published on April 26, 2019 as DOI: 10.1124/dmd.119.087007
This article has not been copyedited and formatted. The final version may differ from this version.

Figure 5.

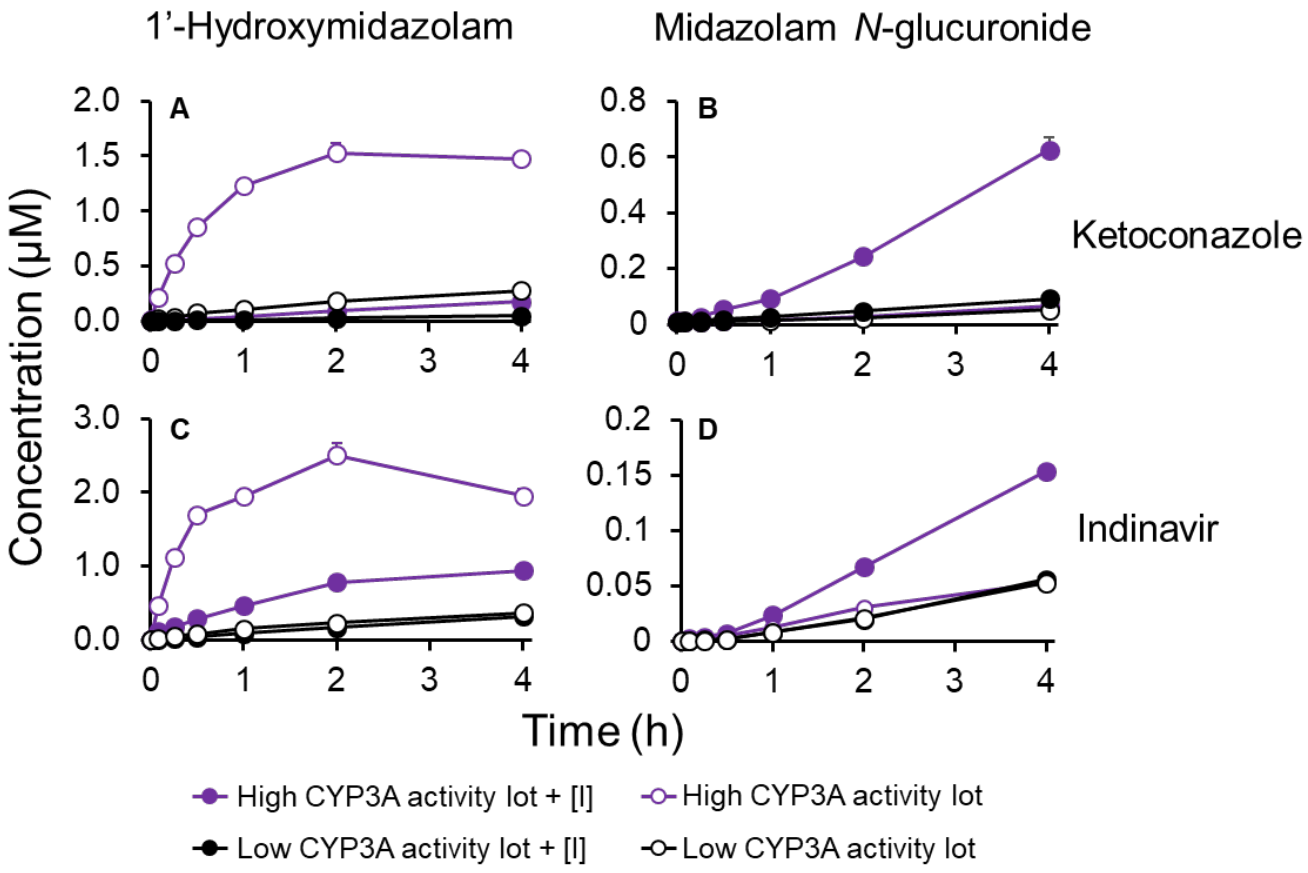

DMD Fast Forward. Published on April 26, 2019 as DOI: 10.1124/dmd.119.087007
This article has not been copyedited and formatted. The final version may differ from this version.

Figure 6.

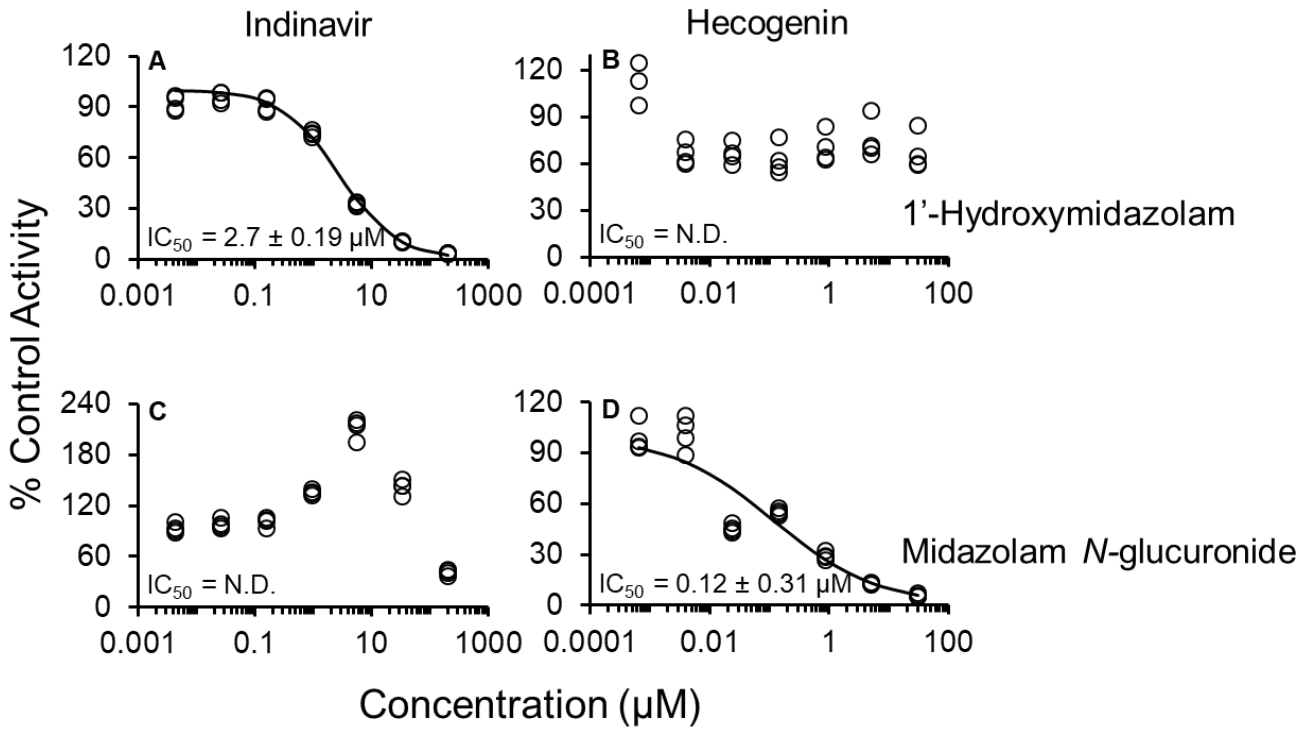

DMD Fast Forward. Published on April 26, 2019 as DOI: 10.1124/dmd.119.087007
This article has not been copyedited and formatted. The final version may differ from this version.

Figure 7.

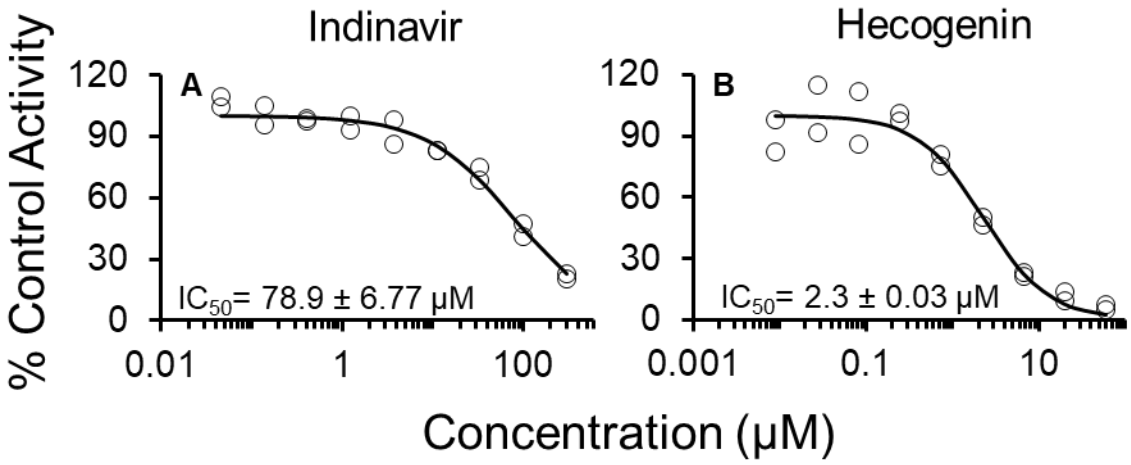

DMD Fast Forward. Published on April 26, 2019 as DOI: 10.1124/dmd.119.087007
This article has not been copyedited and formatted. The final version may differ from this version.

Figure 8.